PROCEEDINGS OF SCIENCE

Recent results in Higgs physics

Emanuele Di Marco[a,*] **on behalf of the ATLAS, CMS collaborations**

[a] *Istituto Nazionale di Fisica Nucleare (INFN), Sezione di Roma-1, Piazzale Aldo Moro n. 2, 00185, Rome, Italy*

E-mail: emanuele.dimarco@roma1.infn.it

This document summarizes recent results from ATLAS and CMS collaborations in the measurements of production cross section, decay rates, and determination of the properties for the Higgs boson, using proton-proton collision data from the LHC Run-2 and Run-3. The focus is on recent results using single Higgs boson production. Updated measurements of its rare processes, as $H \to \mu^+\mu^-$, $t\bar{t}H(H \to c\bar{c})$, and $H \to Z\gamma$ decays are presented, as well as results on double Higgs boson productions, propaedeutical to the determination of the Higgs boson self coupling.

The European Physical Society Conference on High Energy Physics (EPS-HEP2025)
7-11 July 2025
Marseille, France

*Speaker

 ISSN 1824-8039 . Published by SISSA Medialab.

PoS(EPS-HEP2025)027

1. Introduction

In the ten years since the discovery of the Higgs boson by the ATLAS [1, 2] and CMS [3–5] Collaborations, much has been learned about this particle. Most of the major production modes and decay channels have been observed, and with the proton-proton collision data collected during Run-2 (2015–2018) and Run-3 (2022-2024) of the LHC it is possible to probe the cross sections and properties with increasing precision. The larger datasets allow access to rare decay modes or rare production processes of the Higgs boson. Finally, the current data set is used to search for double Higgs boson production, sensitive to the Higgs self coupling.

2. Higgs Boson Production and Decay Measurements

Measurements of Higgs boson production and decay rates were performed by ATLAS and CMS using up to 140 fb^{-1} of p-p collisions at $\sqrt{s}$ = 13 TeV during Run 2 of the LHC, combining the latest analyses for each process. In the STXS framework, Higgs production is divided into non-overlapping bins (*STXS bins*) defined by event kinematics. Results are reported at *stage 0* for major production modes and *stage 1.2* for finer kinematic subdivisions [6], and interpreted in the coupling modifier and SMEFT frameworks [7]. The combination includes $H \to \gamma\gamma$, $ZZ \to 4\ell$, $WW \to \ell\nu\ell\nu$, $\tau\tau$, $b\bar{b}$, $\mu\mu$, $Z\gamma$, and $H \to$ invisible channels, targeting ggH, VBF, VH, ttH, and tH production. Off-shell Higgs analyses constrain the total decay width directly. The overall signal strength μ is consistent with the Standard Model (SM) within 5–6%, dominated by theoretical uncertainties. STXS measurements are consistent with the SM within 6–18%, with significant improvements in WH, ZH, and $t\bar{t}H + tH$ uncertainties of 30%, 20%, and 40%, respectively. ATLAS measures branching fractions for the main decays ($\gamma\gamma$, ZZ^*, WW^*, $b\bar{b}$, $\tau\tau$) with 8–13% uncertainties, consistent with SM predictions. Relative improvements of 10–20% are achieved in $b\bar{b}$, WW^*, and $\tau\tau$ channels, with 29 cross-section × branching ratio combinations reported. Coupling modifier interpretations yield 5–12% uncertainties for W, Z, t, b, and τ couplings, and 25% for the muon. The charm coupling is constrained with $^{+1.6}_{-3.8}$, roughly doubling previous precision. The measured production cross-sections, assuming SM branching fractions, are shown in Fig. 1 (left), while CMS performs the most granular fit with 97 parameters of interest, one per branching ratio in each STXS bin [8], also shown in Fig. 1 (right). All measurements are found to be in excellent agreement with Standard Model predictions.

3. Higgs Boson Couplings with Second Generation Fermions

With the LHC Run-1 and Run-2 data, the Yukawa interactions of the Higgs boson with third-generation charged fermions have been firmly established through several measurements involving H $\to b\bar{b}$ decays. In contrast, the corresponding coupling to second-generation fermions has not yet been conclusively observed. Within the SM, the Higgs boson interactions uniquely distinguish between fermion generations.

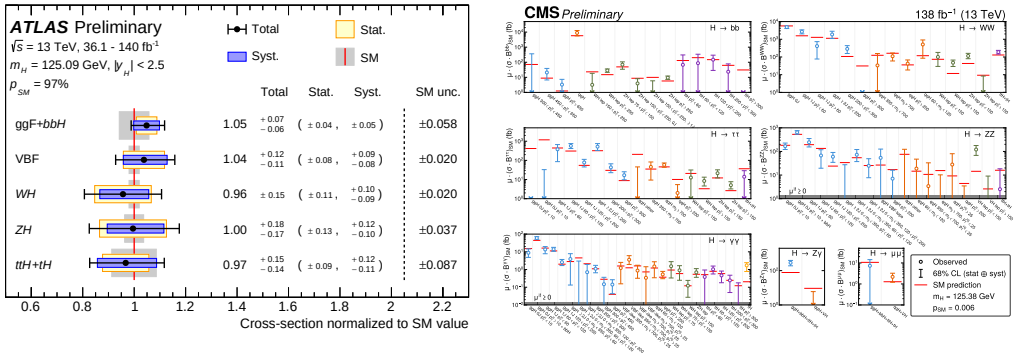

Figure 1: Left: observed cross sections values for the main Higgs boson production modes, relative to their SM predictions, as measured in the most recent ATLAS combination [9]. Right: best fit values (white circles) and 68% CL intervals (coloured lines) for the most granular cross section × branching fraction fit in the recent CMS combination [8].

3.1 Higgs boson Decays into Two Muons

The decay of the Higgs boson into two oppositely charged muons, $H \to \mu^+\mu^-$, provides direct sensitivity to the Yukawa coupling of a second-generation fermion. The SM predicts a branching fraction of 2.17×10^{-4} for this process, for $m_H = 125.09$ GeV [10].

An earlier CMS measurement in this channel provided an observed (expected) significance of 3.0σ (2.5σ). The new search from ATLAS presented here used data recorded during the LHC Run-3, corresponding to an integrated luminosity of 165 fb^{-1} at $\sqrt{s} = 13.6$ TeV, and then combined with the results from Run 2 [11]. The reconstruction of this final state relies on the identification of muons originating from the $H \to \mu^+\mu^-$ decay, as well as additional particles produced in association with the Higgs boson candidate. These include other muons, electrons, photons, jets, and neutrinos, the latter being inferred from the presence of missing transverse momentum, $p_{\mathrm{T}}^{\mathrm{miss}}$. The main event selection requirements are designed to ensure accurate reconstruction and optimal separation of signal and background processes.

Events passing the baseline selection are classified into 23 exclusive categories optimized to distinguish between background processes and the various Higgs boson production mechanisms: $t\bar{t}H$, VH, VBF, and ggF. Multivariate classifiers are employed to enhance signal sensitivity, utilising variables which exploit the kinematic properties of final-state particles. The dominant background arises from Drell–Yan production, with additional contributions from diboson, $t\bar{t}$, single-top, and rarer electroweak processes. Background normalization is determined from data sidebands in $m_{\mu\mu}$ = 110 GeV – 120 GeV and 130 GeV – 160 GeV. Signal extraction is performed using a binned maximum-likelihood fit to the $m_{\mu\mu}$ distribution in the range 110 GeV – 160 GeV. The signal is modeled by a double-sided Crystal Ball function with a mass resolution of 2.8 GeV – 3.2 GeV. The observed mass spectrum, together with the superimposed likelihood fit, is shown in Fig. 2 (left). The dominant systematic uncertainty arises from background modeling, followed by theoretical and muon-related sources. The fit to the observed $m_{\mu\mu}$ spectra yields a best-fit signal strength of $\mu = 1.6 \pm 0.6$, corresponding to an observed (expected) significance of 2.8 (1.8) σ. Combining these results with the full Run 2 dataset increases the observed (expected) significance to 3.4 (2.5) σ,

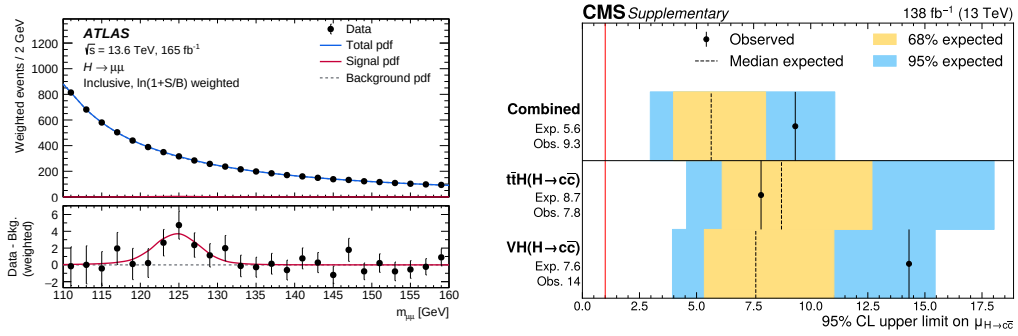

Figure 2: Left: S/B weighted observed dimuon invariant mass spectrum in the ATLAS Run-3 data, combining all analysis categories [11]. Right: the 95% CL upper limits on $\mu_{t\bar{t}H(H\to c\bar{c})}$ for the CMS analysis [12]. The blue and yellow bands indicate the expected 68% and 95% CL regions, respectively, under the background-only hypothesis.

corresponding to a branching fraction of $\mathcal{B}(H \to \mu^+\mu^-) = (3.0 \pm 0.9) \times 10^{-4}$, consistent with the SM expectation.

3.2 Higgs Boson Decays into c-quark Pairs

A search for Higgs boson decays into a charm quark–antiquark pair, $H \to c\bar{c}$, has been performed by CMS using the full LHC Run-2 data [12]. The analysis targets Higgs boson production in association with a top quark pair ($t\bar{t}H$), performed simultaneously with the measurement of $H \to b\bar{b}$. The analogous $t\bar{t}Z$ processes with $Z \to c\bar{c}$ and $Z \to b\bar{b}$ decays are used for validation. The event reconstruction employs advanced machine learning algorithms, including ParticleNet [13] for jet flavour identification and the Particle Transformer [14] for event classification. Events are categorized according to lepton multiplicity and heavy-flavour content to enhance signal purity. Backgrounds from $t\bar{t}$+jets, $t\bar{t}W$, and single-top production are modelled using NLO simulations with flavour-dependent corrections constrained by control regions in data. Signal extraction is performed via a simultaneous binned likelihood fit to the Particle Transformer discriminants. The measured signal strengths are $\mu_{t\bar{t}H(H\to b\bar{b})} = 0.91^{+0.26}_{-0.22}$ and $\mu_{t\bar{t}H(H\to c\bar{c})} = -1.6 \pm 4.5$, with an observed (expected) significance of 4.4 (4.5) σ for $t\bar{t}H(H \to b\bar{b})$. No excess is observed in the $t\bar{t}H(H \to c\bar{c})$ channel, leading to an observed (expected) 95% confidence level upper limit of $\mu_{t\bar{t}H(H\to c\bar{c})} < 7.8\ (8.7^{+4.0}_{-2.6})$.

Combining this result with previous searches in the VH production mode yields the most stringent constraint to date on the charm Yukawa coupling, with an observed (expected) 95% CL bound of $|\kappa_c| < 3.5\ (2.7)$, assuming SM production cross sections. The corresponding upper limits in the two production modes, as well as their combination are shown in Fig. 2 (right).

4. Rare Decay Channels and Production Modes

4.1 Decay Into a Z Boson and a Photon

Within the SM, the Higgs boson decay to a Z boson and a photon ($H \to Z\gamma$) occurs via loop-induced processes, yielding a predicted branching ratio of $\mathrm{BR}(H \to Z\gamma) = (1.54^{+0.10}_{-0.11}) \times 10^{-3}$

for $m_H = 125.09$ GeV, similar to $H \to \gamma\gamma$. Extensions of the SM can modify this rate through new particles in the loops, making the ratio BR($H \to Z\gamma$)/BR($H \to \gamma\gamma$) a sensitive probe of new physics. Observation of $H \to Z\gamma$ would complete the set of Higgs decays into electroweak boson pairs, consolidating its role in electroweak symmetry breaking. The $Z(\to \ell\ell)\gamma$ final state ($\ell = e, \mu$) offers the best sensitivity, providing full kinematic reconstruction and excellent invariant-mass resolution.

The earlier combination of ATLAS and CMS Run-2 searches at $\sqrt{s} = 13$ TeV with 140 fb^{-1} yielded a first evidence for $H \to Z\gamma$ at $3.4\,\sigma$, $\mu = 2.2 \pm 0.7$. The results presented here include a Run-3 search using 165 fb^{-1} at $\sqrt{s} = 13.6$ TeV [15]. Improvements include increased production cross-section, larger datasets, optimized p_T thresholds, and 13 event categories, including a new multi-lepton category. Twelve categories use an improved multivariate classifier to enhance sensitivity. A simultaneous fit to the $Z\gamma$ invariant mass across all categories extracts the $H \to Z\gamma$ signal, which is combined with Run-2 results to further increase sensitivity. The $H \to Z\gamma$ signal is extracted via an unbinned maximum-likelihood fit to $m_{Z\gamma}$ distributions across all Run-3 categories, including nuisance parameters for systematic uncertainties. The measured signal strength is $\mu = 0.9^{+0.7}_{-0.6}$, compatible with the SM expectation $\mu_{\text{exp}} = 1.0 \pm 0.7$, with observed (expected) significance 1.4 (1.5) σ. Statistical uncertainties dominate, while background modelling is the largest systematic. Run-3 improves expected significance by 28% relative to Run-2, due to optimized selection, categorisation, and larger dataset at $\sqrt{s} = 13.6$ TeV. Run-3 results are combined with Run-2, correlating theoretical but not most of the experimental uncertainties. The combined fit gives $\mu = 1.3^{+0.6}_{-0.5}$ with a significance of $2.5\,\sigma$ ($1.9\,\sigma$ expected), compatible with Run-2 (p-value=0.33). This provides the most stringent sensitivity to date for $H \to Z\gamma$ branching fraction. Assuming SM production, the observed branching fraction is $(2.0^{+0.9}_{-0.8}) \times 10^{-3}$, consistent with the SM prediction of $(1.54^{+0.10}_{-0.11}) \times 10^{-3}$.

4.2 Electroweak VVH Production

VVH production via vector boson scattering (VBS) probes the Higgs self-coupling (κ_λ) and VVHH quartic coupling (κ_{2V}), with a SM LO cross section of 1.77 fb at $\sqrt{s} = 13$ TeV. The search [16] uses 138 fb^{-1} of CMS data (2016–2018), targeting $H \to b\bar{b}$ decays in all-hadronic, semileptonic, and dileptonic channels. Higgs boson and vector boson decay products are reconstructed as large-cone jets, with forward-backward VBS jet pairs exploited. Channel orthogonality is ensured via lepton and jet multiplicities, Z mass windows, and specific selections; multivariate techniques (DNNs, BDTs) are used for signal discrimination. Backgrounds are estimated through extrapolation from control regions; signal extraction uses simple counting in the signal region, subtracting the background prediction. Systematic uncertainties include factorization/renormalization scales, PDFs, jet/lepton reconstruction, b-tagging, boosted resonance tagging, and integrated luminosity. The 95% CL intervals are $\kappa_{2V} \in [0.40, 1.60]$, $\kappa_{2W} \in [0.17, 1.84]$, $\kappa_{2Z} \in [-0.37, 2.38]$, with two-dimensional likelihood scans further constraining anomalous quartic couplings, as shown in Fig. 3 (right).

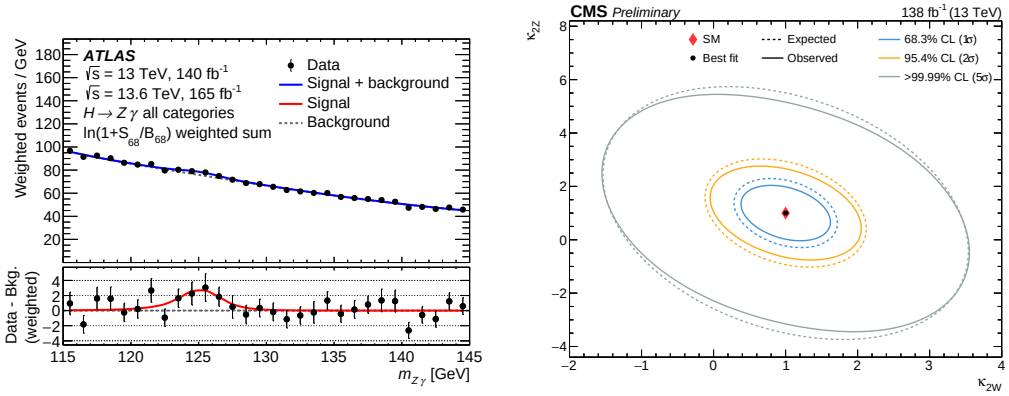

Figure 3: Left: $Z\gamma$ invariant mass distributions of S/B weighted data for the combined Run-2 and Run-3 ATLAS dataset [15]. The black points represent the data, while the signal-plus-background fit (solid blue curve) and the background model (dashed line) are overlaid. Right: observed (solid line) and expected (dashed line) 1, 2 and 5 σ exclusion regions in the $\kappa_{2W} - \kappa_{2Z}$ plane from the CMS $VVH(H \to b\bar{b})$ analysis using Run-2 data [16].

5. CP Properties

The Higgs boson spin-parity is consistent with $J^{PC} = 0^{++}$, excluding nonzero spin assignments, though small anomalous couplings to electroweak bosons (HVV) or gluons (Hgg) remain possible. CP-violating effects in Higgs boson couplings to fermions (Hff) and gluons, probed via ttH production and $H \to \tau\tau$ decays, provide complementary insights and indirect searches for BSM phenomena, with current constraints limited in sensitivity. New results on this topic are presented here, using $H \to \gamma\gamma$ decay channel (CMS) and $H \to \tau^+\tau^-$ channel (ATLAS), using the LHC Run-2 data.

5.1 Anomalous Higgs Boson Couplings in $H \to \gamma\gamma$ Decay

In the CMS analysis of the $H \to \gamma\gamma$ channel [17], the formalism of previous CMS analyses is adopted to study anomalous Higgs boson couplings in HVV and Hgg interactions. The HVV amplitude is described by three tensor structures with coefficients expanded in q^2/Λ_1^2, including potential CP-odd contributions [18]. In the SM, only the tree-level contributions proportional to a_1 are nonzero, with other couplings considered anomalous or loop-induced. CP-odd terms a_3 lead to CP violation when combined with CP-even couplings. Effective fractional cross sections f_{ai} are measured instead of direct couplings, canceling many uncertainties. The analysis uses $H \to \gamma\gamma$ decays, measuring one anomalous coupling at a time, and optionally up to four simultaneously.

The sensitivity to HVV couplings is obtained from VBF and VH production, with preselected events categorized to enhance signal discrimination, though ggH and ttH events also populate these categories. VBF categories require at least two jets with $m_{jj} > 350$ GeV, leading jet $p_T > 40$ GeV, subleading jet $p_T > 30$ GeV, and $|\eta| < 4.7$, then divided using dedicated matrix element or multivariate discriminants, optimized for CP-odd sensitivity. Five VBF tags retain optimal sensitivity to anomalous couplings f_{a3}, $f_{\Lambda 1}$, $f_{Z\gamma}^{\Lambda 1}$, and f_{a2}, with inputs including jet kinematics and photon angular variables. $V(\text{had})H$ categories select two jets with $60 < m_{jj} < 120$ GeV and use a DNN outputs to define five categories, including two BSM-dominated tags. $V(\text{lep})H$ categories target

$Z(\ell\ell)H$, $W(\ell\nu)H$, and $Z(\nu\nu)H$ events, using lepton and $p_{\mathrm{T}}^{\mathrm{miss}}$ selections combined with STXS and BSM-trained BDTs. Expected signal and background yields are determined for each category, with high-purity tags targeting maximal anomalous coupling contributions. This categorization strategy allows a simultaneous fit across all reconstructed categories, constraining both SM and BSM HVV contributions in situ. The effective cross section ratios $\vec{f} = f_{a2}, f_{a3}, f_{\Lambda 1}, f_{\Lambda 1}^{Z\gamma}$ are extracted via a simultaneous fit to the $m_{\gamma\gamma}$ distributions across all categories. In the HVV analysis, constraints are placed on the CP-violating parameter f_{a3} and CP-conserving parameters $f_{a2}, f_{\Lambda 1}, f_{\Lambda 1}^{Z\gamma}$. The resulting 68% CL limits are $f_{a3} = (0.00^{+0.39}_{-0.39}) \times 10^{-4}$, $f_{a2} = (-0.81^{+0.65}_{-2.0}) \times 10^{-4}$, $f_{\Lambda 1} = (-0.014^{+0.032}_{-0.14}) \times 10^{-4}$, $f_{\Lambda 1}^{Z\gamma} = (0.83^{+1.5}_{-0.92}) \times 10^{-4}$, representing some of the most stringent limits to date. One example of the resulting likelihood curve for the f_{a3} parameter for HVV couplings is shown in Fig. 4 (left).

5.2 CP Measurements in $H \to \tau^+\tau^-$ Decays

ATLAS has performed a search for CP violation in the VBF production of the Higgs boson using the $H \to \tau^+\tau^-$ decay, which provides a high signal-to-background ratio and efficient reconstruction [19]. The study uses 140 fb^{-1} of Run 2 pp collisions. The Optimal Observable method, incorporating full multidimensional production phase space information, is employed, with additional CP-odd observables used for comparison. The analysis benefits from updated background estimates and novel machine learning techniques, with results interpreted in the HISZ and Warsaw bases. Events with at least two jets and a Higgs candidate decaying via $H \to \tau^+\tau^-$ are targeted. Three τ decay channels are considered: fully hadronic ($\tau_{\mathrm{had}}\tau_{\mathrm{had}}$), semileptonic ($\tau_{\mathrm{lep}}\tau_{\mathrm{had}}$), and leptonic ($\tau_{\mathrm{lep}}\tau_{\mathrm{lep}}$), with same-flavor leptonic decays rejected to reduce $Z \to ee/\mu\mu$ backgrounds. CP parameters are extracted via a binned maximum-likelihood fit over SRs and CRs, with signal templates reweighted from SM VBF Higgs predictions. Signal regions are binned in the Optimal Observable, with one CR per SR to constrain $Z \to \tau^+\tau^-$. A common normalization factor is applied to signal, equal to ($\mu_{\mathrm{VBFH}} = 0.87^{+0.14}_{-0.13}$) as well as for the background, with top background constrained in the leptonic channel. Fits are performed separately for each decay channel and combined, treating experimental and theoretical uncertainties as correlated. No significant deviation from the SM CP-even Higgs boson is observed. The parameter $\tilde{d}$ is constrained to $[-0.012, +0.044]$, and the parameter $c_{H\tilde{W}}$ to $[-0.24, +0.83]$ for the BSM scale $\Lambda = 1$ TeV, including linear and quadratic terms. These results are competitive with other decay modes, such as $H \to ZZ^*$ and $H \to \gamma\gamma$ (Fig. 4, right).

6. Higgs Boson Pair Production in $b\bar{b}\gamma\gamma$ Final State

A key goal of the LHC programme and an intense line of current research is probing the Higgs potential and electroweak symmetry breaking. In the SM, the Higgs potential is fully determined by the vacuum expectation value $v \approx 246$ GeV and $m_H \approx 125$ GeV. Deviations from the SM form would signal new physics, with the trilinear coupling κ_λ accessible via Higgs pair production (HH). Gluon-gluon fusion (ggF) and vector-boson fusion (VBF) are the main HH production modes, with contributions from HHH, t-quark Yukawa, VVH, and $VVHH$ vertices. Destructive interference between diagrams makes sensitivity to κ_λ largest near the HH production threshold, with cross sections $\sigma_{HH}^{\mathrm{ggF}} \sim 30$ fb and $\sigma_{HH}^{\mathrm{VBF}} \sim 1.7$ fb at 13 TeV. A new analysis from ATLAS [20], using

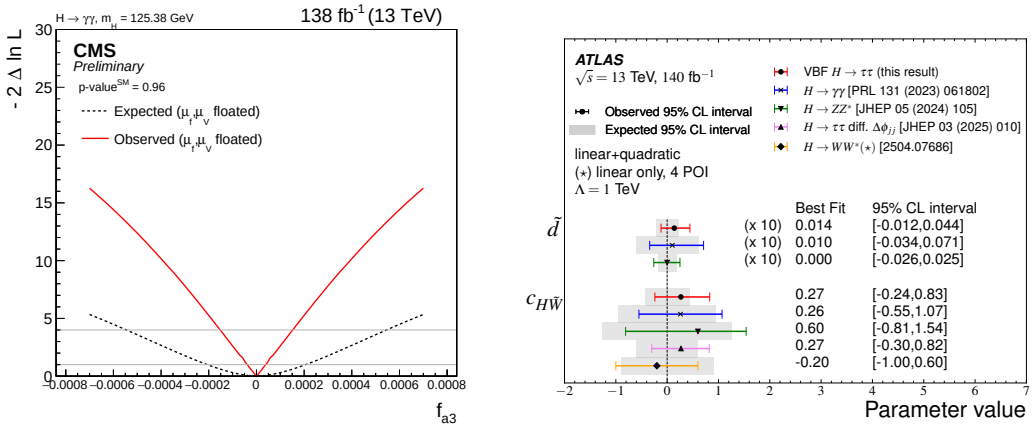

Figure 4: Left: likelihood scan for the expected and observed constraints of the HVV coupling parameter f_{a3}, with p-value$_{\mathrm{SM}} = 0.96$ from the CMS anomalous couplings analysis using $H \to \gamma\gamma$ decay [17]. Right: comparison of results of the present ATLAS $H \to \tau^+\tau^-$ analysis with the $H \to ZZ^* \to 4\ell$ analysis $H \to \gamma\gamma$ VBF measurements for the CP parameters $c_{H\tilde{W}}$ and $\tilde{d}$. The data points show the observed results, and the uncertainty bands correspond to the 95% CL interval [19].

140 fb^{-1} of Run-2 and 168 fb^{-1} of Run-3 data, targets the $HH \to b\bar{b}\gamma\gamma$ channel, which has low branching ratio (0.26%) but excellent diphoton mass resolution and high efficiency near threshold. Improvements include transformer-based b-tagging (GN2) and a kinematic fit.

The analysis selects events containing exactly two well-reconstructed photons and at least two b-jets candidates. This selection includes di-photon triggers, tight photon identification, isolation requirements, and at least two b-tagged jets. Jets are reconstructed with the anti-k_t algorithm and novel corrections improve the $b\bar{b}$ and $b\bar{b}\gamma\gamma$ invariant mass resolution by up to 46%.

Events are categorized into high- and low-mass regions based on the modified four-body invariant mass $m^*_{b\bar{b}\gamma\gamma}$. Boosted Decision Trees (BDTs) are used to separate signal from background, defining exclusive categories. Signal and background $m_{\gamma\gamma}$ distributions are modeled analytically, with non-resonant backgrounds estimated using data-driven methods. Systematic uncertainties arise from photon and jet calibration, b-tagging, luminosity, and theoretical predictions, while statistical uncertainties dominate.

The measured Higgs pair signal strength is $\mu_{HH} = 0.9^{+1.3}_{-1.0}(\mathrm{stat.})^{+0.6}_{-0.5}(\mathrm{syst.})$, corresponding to a 95% CL upper limit of $\mu_{HH} < 3.8$. Constraints on the Higgs self-coupling and quartic couplings are $-1.7 < \kappa_\lambda < 6.6$ and $-0.5 < \kappa_{2V} < 2.6$, respectively, improving upon previous results. The Fig. 5 show the reconstructed diphoton mass for the selected events, with the fit superimposed, and the observed 95% CL upper limit on the signal strength of the process.

7. Summary

Recent studies by the ATLAS and CMS collaborations have presented combinations of measurements of simplified template cross sections, measurements for the second generation Yukawa couplings, and searches of rare productions or decay modes for the Higgs boson. Moreover, investigations of the CP properties both with vector bosons or fermions have been performed. Investigations on the self-coupling of the Higgs boson, crucial for the determination of the Higgs

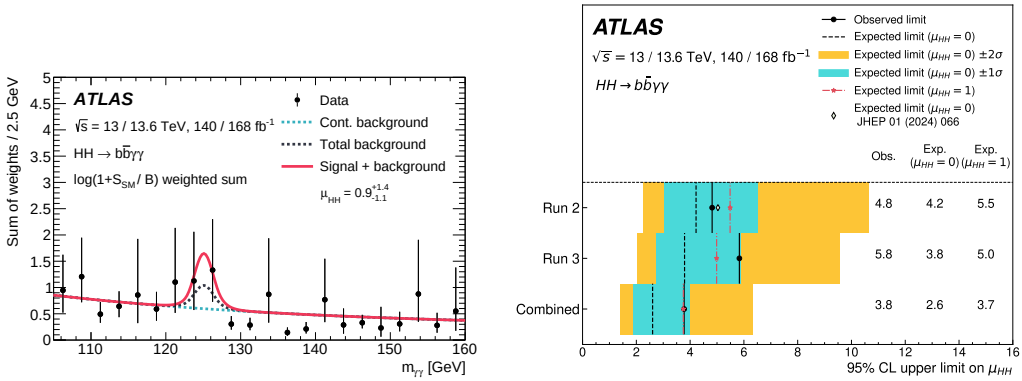

Figure 5: Left: S/B weighted di-photon invariant mass distribution in 308 fb^{-1} of ATLAS data, with the superimposed likelihood fit. The lines show the fit results for the continuum background only (light dotted), adding single Higgs boson backgrounds (black dotted) and the full fit (solid). Right:the 95% CL upper limits on the $HH \to b\bar{b}\gamma\gamma$ signal strength, obtained with the Run-2 and Run-3 data as well as their combination in the ATLAS analysis. [20].

potential, have been also performed with increasing precision. These analyses utilized the full Run-2 dataset and the first part of Run-3 of the LHC, yielding results consistent with Standard Model expectations. Ongoing analyses continue to exploit this growing dataset. Consequently, increasingly precise determinations of Higgs boson production cross sections and properties are anticipated in the near future.

References

[1] ATLAS collaboration, *The ATLAS Experiment at the CERN Large Hadron Collider*, *JINST* **3** (2008) S08003.

[2] ATLAS collaboration, *Observation of a new particle in the search for the Standard Model Higgs boson with the ATLAS detector at the LHC*, *Phys. Lett. B* **716** (2012) 1 [1207.7214].

[3] CMS collaboration, *The CMS Experiment at the CERN LHC*, *JINST* **3** (2008) S08004.

[4] CMS collaboration, *Observation of a New Boson at a Mass of 125 GeV with the CMS Experiment at the LHC*, *Phys. Lett. B* **716** (2012) 30 [1207.7235].

[5] CMS collaboration, *Observation of a New Boson with Mass Near 125 GeV in pp Collisions at $\sqrt{s} = 7$ and 8 TeV*, *JHEP* **06** (2013) 081 [1303.4571].

[6] LHC Higgs Cross Section Working Group collaboration, S. Heinemeyer, ed., *Handbook of LHC Higgs Cross Sections: 3. Higgs Properties*, CERN Yellow Reports: Monographs, CERN (2013), 10.5170/CERN-2013-004.

[7] I. Brivio and M. Trott, *The standard model as an effective field theory*, *Physics Reports* **793** (2019) 1.

[8] CMS collaboration, *Combined measurements and interpretations of Higgs boson production and decay at $\sqrt{s}$=13 TeV*, Tech. Rep. CMS-PAS-HIG-21-018, CERN, Geneva (2025).

[9] ATLAS collaboration, *Combined measurements of Higgs boson production and decay at $\sqrt{s}$ = 13 TeV using up to 140 fb^{-1} of data collected by the ATLAS Experiment*, Tech. Rep. ATLAS-CONF-2025-006, CERN, Geneva (2025).

[10] S. Dittmaier et al., *Handbook of LHC Higgs Cross Sections: 2. Differential Distributions*, 1201.3084.

[11] ATLAS collaboration, *Evidence for the dimuon decay of the Higgs boson in pp collisions with the ATLAS detector*, 2507.03595.

[12] CMS collaboration, *Simultaneous probe of the charm and bottom quark Yukawa couplings using* $t\bar{t}H$ *events*, Tech. Rep. CMS-HIG-24-018, CERN-EP-2025-202, CERN, Geneva (2025).

[13] H. Qu and L. Gouskos, *ParticleNet: Jet Tagging via Particle Clouds*, *Phys. Rev. D* **101** (2020) 056019 [1902.08570].

[14] H. Qu, C. Li and S. Qian, *Particle transformer for jet tagging*, vol. 162 of *Proceedings of Machine Learning Research*, pp. 18281–18292, PMLR, 17–23 Jul, 2022, https://proceedings.mlr.press/v162/qu22b.html.

[15] ATLAS collaboration, *Search for the Higgs boson decay to a Z boson and a photon in pp collisions at $\sqrt{s}$ = 13 TeV and 13.6 TeV with the ATLAS detector*, Tech. Rep. CERN-EP-2025-155 (7, 2025).

[16] CMS collaboration, *Search for associated production of a Higgs boson and of two vector bosons via vector boson scattering*, Tech. Rep. CMS-PAS-HIG-24-003, CERN, Geneva (2025).

[17] CMS collaboration, *Constraints on anomalous Higgs boson couplings to vector bosons and fermions analyzing the $\gamma\gamma$ final state*, Tech. Rep. CMS-PAS-HIG-24-006, CERN, Geneva (2025).

[18] Y. Gao, A.V. Gritsan, Z. Guo, K. Melnikov, M. Schulze and N.V. Tran, *Spin Determination of Single-Produced Resonances at Hadron Colliders*, *Phys. Rev. D* **81** (2010) 075022 [1001.3396].

[19] ATLAS collaboration, *Probing the Higgs boson CP properties in vector-boson fusion production in the $H \to \tau^+\tau^-$ channel with the ATLAS detector*, Tech. Rep. CERN-EP-2025-127 (6, 2025).

[20] ATLAS collaboration, *Study of Higgs boson pair production in the $HH \to b\bar{b}\gamma\gamma$ final state with 308 fb^{-1} of data collected at $\sqrt{s}$ = 13 TeV and 13.6 TeV by the ATLAS experiment*, Tech. Rep. CERN-EP-2025-140 (7, 2025).